

# Reinforcement learning-based motion imitation for physiologically plausible musculoskeletal motor control

Merkourios Simos

Alberto Silvio Chiappa  
EPFL

Alexander Mathis\*

## Abstract

How do humans move? The quest to understand human motion has broad applications in numerous fields, ranging from computer animation and motion synthesis to neuroscience, human prosthetics and rehabilitation. Although advances in reinforcement learning (RL) have produced impressive results in capturing human motion using simplified humanoids, controlling physiologically accurate models of the body remains an open challenge. In this work, we present a model-free motion imitation framework (KINESIS) to advance the understanding of muscle-based motor control. Using a musculoskeletal model of the lower body with 80 muscle actuators and 20 DoF, we demonstrate that KINESIS achieves strong imitation performance on 1.9 hours of motion capture data, is controllable by natural language through pre-trained text-to-motion generative models, and can be fine-tuned to carry out high-level tasks such as target goal reaching. Importantly, KINESIS generates muscle activity patterns that correlate well with human EMG activity. The physiological plausibility makes KINESIS a promising model for tackling challenging problems in human motor control theory, which we highlight by investigating Bernstein’s redundancy problem in the context of locomotion. Code, videos and benchmarks will be available at <https://github.com/amathislab/Kinesis>.

## 1. Introduction

Understanding human motion is a pivotal scientific challenge that intersects diverse fields such as computer vision, biomechanics, cognitive science, and neuroscience—each offering distinct perspectives toward a comprehensive grasp of this fascinating phenomenon [1, 3, 12, 14, 22, 37, 44, 62, 69]. Recent advancements in computer science have enabled the development of virtual humanoid agents capable of navigating complex terrain, dancing, and interacting with objects [13, 64]. However, these agents are actuated by torque controllers that fail to capture the intricate connec-

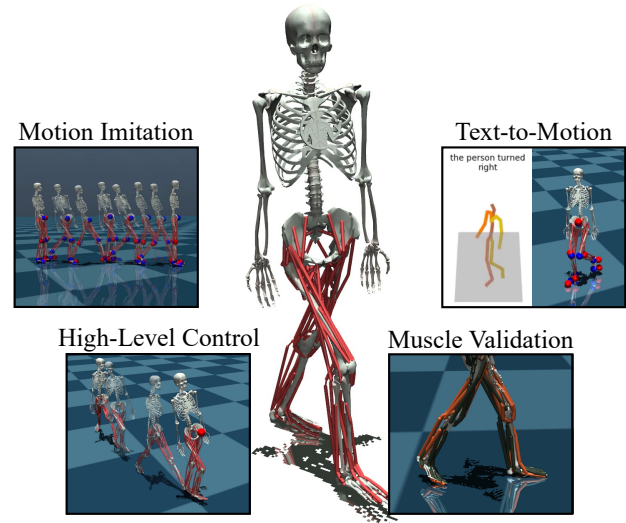


Figure 1. KINESIS is a model-free RL policy for the musculoskeletal control of locomotion. **Top left:** Our policy is trained on a curated set of MoCap data focusing on locomotion, and can successfully imitate unseen motion clips of the same locomotion type. **Top right:** KINESIS can be deployed zero-shot on synthetic text-conditioned motion sequences. **Bottom left:** KINESIS is fine-tuned to a high-level goal target reaching task, and produces human-like motion according to real-time instructions. **Bottom right:** Muscle activity patterns produced during motion imitation (active muscles shown in orange, inactive muscles shown in black) correlate well with human electrophysiology data (EMG).

tions between goal-driven intention, biological motor control, and action. To bridge this gap, it is essential to explore the fundamental mechanism underlying human motor control: the musculoskeletal system [3, 9, 15, 37, 69]. By integrating the constraints and dynamics of human motor control, we can seek to design agents capable of translating cognitive intentions into human-like behaviors.

Recent studies have leveraged reinforcement learning (RL) to achieve significant progress in motion imitation for torque-actuated humanoids. Remarkably, they were able to master extensive motion capture datasets, sometimes exceeding 40 hours [39, 40]. However, the hu-

\*Contact: alexander.mathis@epfl.ch

man musculoskeletal system poses greater challenges due to its non-linear, high-dimensional, and over-actuated nature [3, 14, 15, 37, 62]. Thus, it remains unclear whether techniques effective for simplified humanoid agents will work in this more challenging setting. Additionally, there is a shortage of physiologically accurate, full-body musculoskeletal models that are also fast to simulate. Those that do exist often feature partial muscle actuation [4, 15, 34], which restricts the diversity of achievable movements. Finally, to genuinely model human motion, muscle-based control policies must also strive to replicate the actual muscle activity patterns observed in humans performing analogous movements; it is therefore necessary to validate generated patterns against empirical human data.

In this work, we aim to address the following questions: *Can model-free RL methods for motion imitation be applied to more complex control regimes, such as musculoskeletal models? If so, how realistic are the resulting control policies compared to empirical knowledge about human muscle control?* We propose a comprehensive motion imitation framework that facilitates the development of effective and scalable muscle-based motion control policies. Our contributions are as follows: (1) We develop a motion imitation framework focused on acquiring locomotion skills by extracting suitable clips (of locomotion) from the KIT motion capture dataset [52]. (2) We implement this framework on a full-body, leg-actuated musculoskeletal model with 80 experimentally validated muscles using Mujoco and MyoSuite [4, 66], and we demonstrate that the learned policy achieves high motion tracking performance and high-level controllability through natural language and target-reaching commands. (3) Furthermore, we find that the proposed policy produces physiologically plausible muscle activity patterns, validated by comparisons with human electromyography (EMG) recordings, unlike current state-of-the-art locomotion control policies [23, 58]. (4) We analyze the dimensionality of the learned control policy with a task-aware metric. Our analysis highlights that traditional signal reconstruction-based methods underestimate the complexity of human locomotion.

## 2. Related Work

Table 1. Comparison of related works. MI: Motion imitation. Code: training code. EMG: electromyography validation

Work	MI	Multi-Clip	Full-Body	Code	Metrics	EMG
DEP-RL [58]	✗	N.A.	✗	✓	✓	✗
DynSyn [23]	✗	N.A.	✓	✓	✓	✗
MASS [34]	✓	✗	✓	✓	✓	✗
MuscleVAE [19]	✓	✓	✓	✗	✗	✗
KINESIS	✓	✓	✗	✓	✓	✓

**Control of Humanoid Agents.** Physics-based simulation environments provide a fertile ground for developing human motion control policies through RL. Early works primarily focused on isolated skills and interactive control, but motion imitation soon emerged as a prominent paradigm for complex motor skill acquisition [49–51]. This paradigm has expanded to encompass large-scale, diverse motion repertoires, including several hours of motion capture (MoCap) data [29, 39, 40, 64]. Leveraging the richness of these motion datasets posed significant challenges, which were addressed through techniques such as reference state initialization [45, 49, 55, 61], early termination [48, 49], and progressive learning regimes [39]. Furthermore, several works have integrated motion imitation tasks with variations of adversarial learning to shape motion behavior [50, 51, 63], while recent approaches utilize latent representations to capture the relationships between humanoid states, goals, and actions [29, 40, 74].

For high-dimensional musculoskeletal control, some works have utilized reference motion data [19, 34, 53], whereas others focused on task-oriented learning frameworks [2, 5–9, 30, 47, 58, 59, 76]. To our knowledge, MuscleVAE [19] is the only study that combines a full-body human musculoskeletal model with the motion imitation of various locomotion skills under a unified control policy. Unfortunately, at the time of writing there is no training code available, and there are no reported quantitative performance metrics, so we cannot directly compare MuscleVAE with KINESIS in the considered locomotion tasks. Nevertheless, our method differs substantially from MuscleVAE, as we use an experimentally validated musculoskeletal model, we follow a model-free approach without the need for a world model, we implement text-to-motion control, and we compare to human muscle activity data, with which KINESIS achieves substantial correlation.

**Musculoskeletal Models of the Human Body** Efforts to model the human musculoskeletal system trace back to the Hill-type model, which provided a mathematical formulation of the dynamical properties of muscles [26], and much later of musculotendon units [75]. Since then, many works have incorporated these models into numerical simulations of muscle-based systems. In particular, the OpenSim platform provided an open-source tool for the design of accurate musculoskeletal models of the human body [15, 54]. Unfortunately, although OpenSim is widely used in biomechanics [24, 60, 72], it is computationally costly compared to physics engines that are used in robotics, machine learning and RL [11, 27, 42, 66]. To this end, Lee et al. implemented a full musculoskeletal model in DART [33, 34], and incorporated it into a motor skill task. Similarly, Caggiano et al. developed MyoSuite, a suite of physiologically accurate biomechanical models implemented in Mujoco by

porting models from OpenSim. While MuscleVAE utilizes Lee et al.’s model [19], we opted for MyoS uite due to its broader compatibility with RL-based tasks, physiological validation, its expanding open-source model repository, as well as the prospect of GPU-acceleration support.

**Comparison with human muscle activity.** One benefit of modeling human motion using musculoskeletal models is the potential for generating more realistic and physiologically plausible movement [31, 44]. However, for musculoskeletal models to pose an advantage over simpler alternatives, the control signals must capture something about the muscle activity patterns found in humans, at least within a margin of functional variability. Such a margin is expected when considering the methods which extract empirical muscle data [17]; the verifiability of musculoskeletal models is itself an active research topic [18, 25]. Many works have proposed techniques to predict kinematic and dynamic properties of reference motions, but these properties are estimated rather than generated through control approaches [10, 36, 46, 56, 72]. Electromyography (EMG) signals are a common way to validate the physiological plausibility of biomechanical models fit to motion capture data [16, 25]. In particular, the simulated muscle activity patterns are verified against physiological sequences measured by EMG. This matching is non-trivial, due to the non-linear, high dimensional, and over-actuated nature of biomechanical systems [15, 37]. Some studies have investigated the correspondence between RL-based muscle control and human muscle activity, but for control policies generating a single motion skill at a time [53, 62]. Here, we propose a validation benchmark based on EMG data from human subjects during locomotion [71] that can be applied to any muscle-based control policy modeling leg muscles, and we show that KINESIS significantly outperforms state-of-the-art control policies that use the same musculoskeletal model [23, 58].

### 3. Methods

In this section we describe the musculoskeletal model of the lower body from the MyoS uite library [4], the curated KIT- Locomotion reference dataset, and the motion imitation learning framework.

#### 3.1. Musculoskeletal Model (MyoLeg)

MyoS uite [4] is a library built on top of the Mujoco physics simulator [66], featuring several biologically-accurate models of different human body parts. Among them, MyoLeg is realistic musculoskeletal simulation of the lower part of the human body that is biologically validated against an OpenSim [15] model of the full human body by Rajagopal et al.. Compared to OpenSim, MyoLeg reduces the simulation time by up to three orders of magnitude, making the

motion imitation problem computationally tractable. MyoLeg is actuated by 80 musculotendon units, while the upper body is modeled as a rigid volume with mass. The relevant body markers of the model (pelvis, knees, ankles and toes) closely match the mean human body shape of the SMPL model [38], making the use of MoCap datasets feasible.

#### 3.2. Human Motion Dataset

The human motion clips used in this paper are part of the KIT Motion Dataset [52]. KIT is a collection of MoCap datasets under a unified representation framework, containing a variety of full-body motor skills. Because of our focus on the motion of the lower body, we extracted a locomotion-specific subset of 1084 reference motion sequences (KIT- Locomotion), representing 1.9 hours of MoCap data. We selected motion sequences based on their motion description, using key terms such as ‘walk’, ‘turn’, or ‘run’). We filtered this selection further by evaluating motion categories on feasibility, diversity, and length. In its current form, KIT- Locomotion consists of five broad locomotion skills: (1) *walk*, in which the subject walks forward at varying speeds, (2) *gradual turn*, in which the subject turns to the left or right while walking, (3) *turn in place*, where the subject walks in a straight line, then performs a U-turn and resumes walking, (4) *walk backwards*, where the subject takes backward steps, and (5) *run*, where the subject breaks into a short running stride. We extracted all motions from the AMASS dataset [41], which use the SMPL-H body format [38]. Details about the data processing steps are included in the Supp. Material.

#### 3.3. Motion Imitation

The motion imitation problem can be cast as a Partially-Observable Markov Decision Process (POMDP)  $\mathcal{M} = \langle \mathcal{S}, \mathcal{O}, \mathcal{A}, \mathcal{T}, \mathcal{R}, \gamma, \rangle$ , characterized by the state space  $\mathcal{S}$ , the observation function  $\mathcal{O}$ , the action space  $\mathcal{A}$ , the transition function  $\mathcal{T}$ , the reward function  $\mathcal{R}$  and the discount factor  $\gamma$ . At each time step, an agent interacts with the simulated environment in Mujoco to control the MyoLeg model and track a reference motion. Through the observation function  $\mathcal{O} : \mathcal{S} \rightarrow \mathbb{R}^{309}$ , the environment provides an observation vector  $\mathbf{o}_t \in \mathbb{R}^{309}$ , describing the proprioceptive state of the body. Specifically, the observation vector includes: the height, the tilt and the velocity of the pelvis (8 values), the joint kinematics (position, velocity, angular position and angular velocity for each joint, 234 values), and the feet contact forces (4 values) at time  $t$ , as well as the target reference pose (absolute and relative, 63 values) at time  $t + 1$ . The agent controls the body by specifying a control signal for each of the 80 muscles, represented by a vector  $\mathbf{a}_t \in \mathcal{A} \subset \mathbb{R}^{80}$ . The next state  $\mathbf{s}_{t+1} \in \mathcal{S}$  is determined by the transition function  $\mathcal{P} : \mathcal{S} \times \mathcal{A} \rightarrow \mathcal{S}$ , defined by the physics simulator and the muscle dynamics.

The objective of the agent is to maximize the discounted cumulative reward  $R = \sum_{t=0}^N \gamma^t r_t$ , where  $N$  denotes the termination point of the POMDP and  $\gamma$  denotes the discount factor. The reward  $r_t \in \mathbb{R}$  is the output of the function  $\mathcal{R} : \mathcal{S} \times \mathcal{A} \rightarrow \mathbb{R}$ , which maps the current state  $\mathbf{s}_t$  and action  $\mathbf{a}_t$  into a reward signal. In a motion imitation task, the goal is to reproduce the target movement as faithfully as possible. As in previous motion imitation work [39, 40, 49], we define the imitation component of the reward function as the sum of the negative Euclidean distance between the body’s joint position vector  $\mathbf{p}_t^i$  and the position vector  $\hat{\mathbf{p}}_{t+1}^i$  of the target pose:

$$r_t^{pos} = \exp \left( -k_{pos} \sum_i \|\mathbf{p}_t^i - \hat{\mathbf{p}}_{t+1}^i\|^2 \right). \quad (1)$$

The joints included in the sum are the pelvis, the knees, the ankles, and the toes. We apply an exponential kernel to make the rewards positive and avoid encouraging early termination. The scaling factor  $k_{pos}$  controls the rate at which the reward decreases with higher distance from the target motion frame.

Similarly, we defined a velocity reward:

$$r_t^{vel} = \exp \left( -k_{vel} \sum_i \|\mathbf{v}_t^i - \hat{\mathbf{v}}_{t+1}^i\|^2 \right), \quad (2)$$

where  $\mathbf{v}^i$  and  $\hat{\mathbf{v}}^i$  denote the joint velocities of the same key-points for the skeleton and target pose.

Since the musculoskeletal model is overactuated, with antagonist muscles controlling the same joints, there are infinite sequences of muscle activation that produce the same motion. To distinguish between these solutions and discourage simultaneous co-activation of antagonist muscles, we add L1 and L2 regularization in terms of the expended energy at each time step through the reward component:

$$r_t^e = -\|\mathbf{m}_t\| - \|\mathbf{m}_t\|_2, \quad (3)$$

where  $\mathbf{m}_t$  is the vector containing the muscle activation signals for time step  $t$ . Finally, to address the problem of not tracking the upper body and to encourage stable posture, we include an upright reward component:

$$r_t^{up} = \exp \left( -k_{up} (\theta_{f,t}^2 + \theta_{s,t}^2) \right), \quad (4)$$

where  $\theta_{f,t}$  and  $\theta_{s,t}$  denote the forward and sideways tilt of the pelvis in radians, at time step  $t$ .

The total reward at each time step is a weighted sum of these four components:

$$r_t = w_{pos} r_t^{pos} + w_{vel} r_t^{vel} + w_e r_t^e + w_{up} r_t^{up}. \quad (5)$$

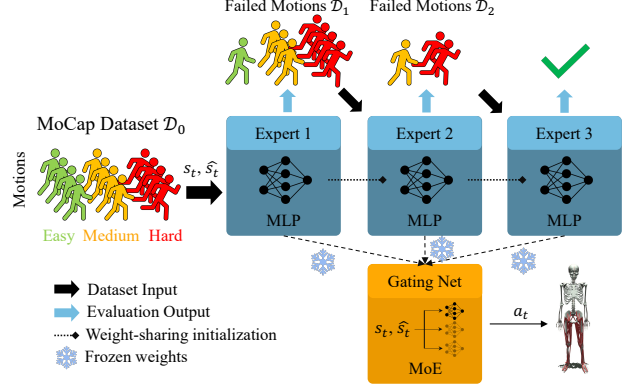


Figure 2. An illustration of the hard negative mining strategy. The first policy network (expert) is trained on the entire dataset, containing five locomotion skills of varying difficulty (here denoted as easy, medium, and hard). After a given number of training epochs, the motions that the first expert successfully imitates are removed from the dataset, and the reduced dataset is used to train a new copy of the expert. The process repeats until the dataset is empty. Finally, a MoE gating network is trained to select the appropriate expert for a specific time step, given the current proprioceptive state and target pose.

**Muscle actuation via PD controllers.** We follow an indirect control scheme, in which the policy output  $\mathbf{a}_t \in \mathbb{R}^{80}$  represents the desired next-step muscle lengths [19, 34, 39]. A proportional-derivative (PD) controller is responsible for finding the force which a muscle should apply for the joint to reach the desired position, according to the equation:

$$F_i = F_i^{\text{peak}} (k_p (a_i - l_i) - k_d v_i), \quad (6)$$

where  $i$  denotes the muscle index,  $F_i^{\text{peak}}$  denotes the maximum force that the muscle can exert,  $l$  denotes the current muscle length,  $v$  denotes current muscle velocity, while  $k_p$  and  $k_d$  are scaling factors that are empirically determined and remain fixed.

To convert muscle force into muscle activity  $\mathbf{m}_t \in \mathbb{R}^{80}$ , we use the force-length-velocity relationship:

$$m_i = \frac{F_i - F_P(l_i)}{F_L(l_i) F_V(v_i)}, \quad (7)$$

where  $F_P$  denotes the force exerted by the muscle’s passive element as a function of its length,  $F_L$  denotes the active isometric force exerted by the muscle as a function of its length, and  $F_V$  denotes the active force exerted by a maximally activated muscle at its resting length, as a function of its velocity. These parameters are provided in MyoLeg.

### 3.4. Reinforcement Learning

In RL, the agent interacting with the environment is defined by the policy  $\pi(\mathbf{a}_t | \mathbf{o}_t)$ , which specifies the conditional

Table 2. Quantitative motion imitation results on the KIT-LoComotion dataset, partitioned into locomotion skills. The Train and Test subsets contain 975 and 109 MoCap sequences, respectively. Mean and SEM for N=10 evaluation runs.

Skill	KIT-LoComotion Train			KIT-LoComotion Test		
	Frame Coverage $\uparrow$	Success $\uparrow$	$E_{MPJPE} \downarrow$	Frame Coverage $\uparrow$	Success $\uparrow$	$E_{MPJPE} \downarrow$
Walk	98.01 $\pm$ 0.09 %	94.86 $\pm$ 0.23 %	46.37 $\pm$ 0.15	97.02 $\pm$ 0.33 %	90.65 $\pm$ 0.96 %	47.07 $\pm$ 0.36
Gradual Turn	99.04 $\pm$ 0.13 %	96.80 $\pm$ 0.31 %	46.29 $\pm$ 0.15	99.13 $\pm$ 0.21 %	97.27 $\pm$ 0.67 %	47.42 $\pm$ 0.41
Turn in Place	96.83 $\pm$ 0.18 %	85.56 $\pm$ 0.68 %	46.36 $\pm$ 0.16	94.69 $\pm$ 0.51 %	76.67 $\pm$ 2.07 %	47.34 $\pm$ 0.31
Walk Backwards	99.49 $\pm$ 0.14 %	96.71 $\pm$ 0.68 %	46.21 $\pm$ 0.18	98.15 $\pm$ 1.75 %	95 $\pm$ 4.74 %	48.16 $\pm$ 0.24
Run	99.91 $\pm$ 0.03 %	98.94 $\pm$ 0.23 %	46.36 $\pm$ 0.16	99.41 $\pm$ 0.26 %	97.73 $\pm$ 0.72 %	47.34 $\pm$ 0.31
Total	98.45 $\pm$ 0.06 %	94.31 $\pm$ 0.21 %	46.33 $\pm$ 0.15	97.71 $\pm$ 0.11 %	91.47 $\pm$ 0.37 %	47.31 $\pm$ 0.34

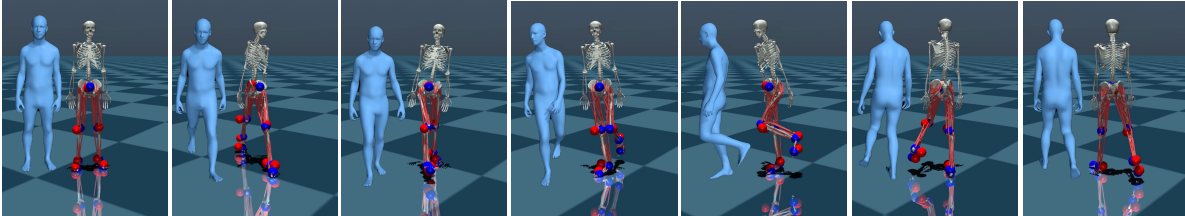


Figure 3. The musculoskeletal model is imitating a “Turn in Place” motion; a rendering of the reference motion is shown on the left.

distribution over actions  $a_t \in \mathbb{R}^{80}$  given an observation  $\mathbf{o}_t \in \mathbb{R}^{309}$ . For training, we apply the motion imitation approach by Luo et al., using a training set  $\mathcal{D}$  with reference motion sequences, including global translation and local joint rotations. During simulation, body positions are extracted from the skeletal model, and velocities and angular velocities are computed via finite differences.

Training episodes begin by sampling a random reference motion from  $\mathcal{D}$  and a random starting frame, setting the musculoskeletal model to the reference state, and initiating environment dynamics. The distance between the reference frame and the model is computed as the episode progresses. If any tracked keypoint deviates more than 0.15 meters from its reference, the episode ends early; otherwise, it concludes at the end of the sequence without further reward, and a new motion is sampled.

### 3.5. Model architecture

We model the policy function with a 6-hidden layer [2048, 1536, 1024, 1024, 512, 512] multilayer perceptron (MLP) [39]. The control policy  $\pi_\theta(\mathbf{a}_t|\mathbf{o}_t) = \mathcal{N}(\mu(\mathbf{o}_t, \theta), \Sigma)$  is a multivariate Gaussian distribution with a covariance matrix  $\Sigma$  and mean  $\mu(\mathbf{o}_t, \theta)$ , where  $\theta$  represents the learned policy network parameters. The policy is trained using proximal policy optimization (PPO) and Lattice, an exploration method that is adapted for high-dimensional control [8, 57] (see Supp. Material for more details). We use the same MLP architecture for modeling the value function.

**Latent time-correlated exploration.** MyoLeg contains actuators which produce a correlated effect on the model’s behavior. To increase the efficiency of policy exploration and to avoid scenarios where random perturbations in different actuators cancel each other out, we employ latent time-correlated exploration (Lattice) [8]. Lattice is a method to inject noise into the latent state of the policy network, so that the learned correlations across actuators shape the policy’s covariance matrix, promoting more effective exploration. Previous experiments in musculoskeletal control using Lattice have shown superior performance compared to unstructured action noise [8, 9, 21].

**Hard negative mining.** The agent must generate a diverse array of control plans to successfully imitate the reference motions. However, the policy required for one motion sequence may be incompatible with policies learned for other motions. To address this, we follow Luo et al. and we employ an ensemble policy based on negative hard mining (Figure 2) [39, 40]. In more detail, the training phase begins by sampling motions from the entire training dataset. When the imitation success rate reaches a plateau, we identify and isolate the motion sequences that the policy fails on. We then initialize a copy of the policy with the currently-learned weights, and we begin a new round of training using only the isolated motion sequences. We continue this process until there are no failed motion sequences left.

**Mixture of experts.** Ultimately, we obtain three different experts. To combine these policy networks into a single, universal policy, we freeze their parameters and train

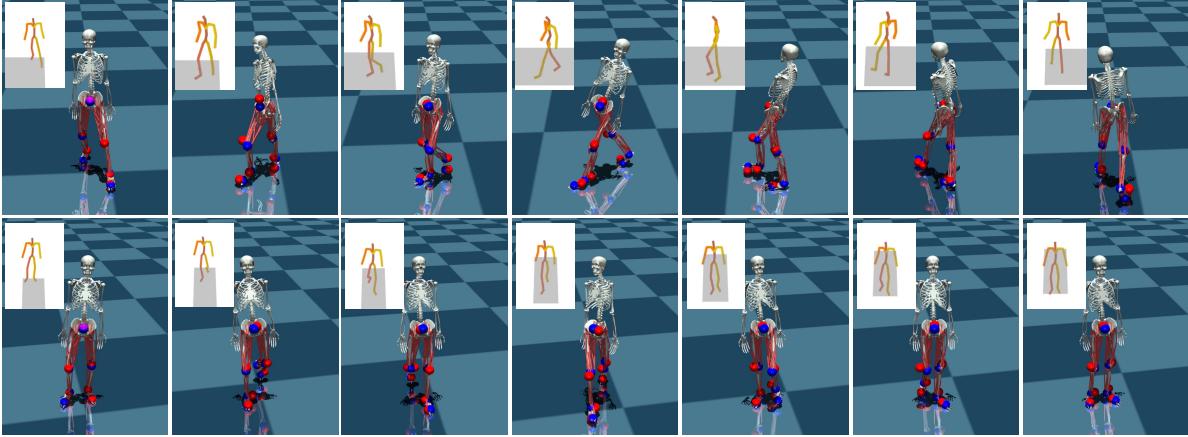


Figure 4. The musculoskeletal model is imitating synthetic motions generated with MDM [65]. Generated trajectories are shown on the top left. **Top:** “The person turned right”. **Bottom:** “The person walked forward”.

a Mixture-of-Experts (MoE) model on the entire training set [28]. The MoE network is a three-layer [1024, 512, 256] MLP that takes as input the current observable state and outputs a vector  $\hat{\mathbf{a}}_t \in \mathbb{R}^n$  that determines which expert’s output will be used to actuate the model. We use a softmax transformation so that  $\hat{a}_t^i$  denotes the probability of using the  $i$ ’th expert’s output as the selected action. Essentially, the MoE network acts as a gating mechanism that stochastically selects an expert based on the current observations.

### 3.6. Text to Motion

A key goal of modeling motion is to complete the behavior loop by incorporating high-level planning and interaction with the environment. We propose to leverage language. To achieve this, we leverage Human Motion Diffusion Model (MDM) to transform the motion imitation task into a text-conditioned motion generation task [65]. The model generates motion sequences as keypoints that align with the SMPL model, which is perfectly aligned with the dimensions of our model’s skeleton. We extract the necessary kinematic properties from the generated motions and initiate the motion imitation task, evaluating the musculoskeletal model in a zero-shot manner.

## 4. Results: Acquiring a motor repertoire

**Implementation Details.** We used three motor experts to minimize network complexity while capturing a significant portion of the motion repertoire. The entire training process took around 10 days on a single NVIDIA A100 GPU and 128 CPU threads, including the MoE policy and the high-level goal finetuning. We used 128 parallel environment instances, training the first expert for 10’000 epochs, the two subsequent experts for 5’000 epochs, and 1’800 epochs for the gating network (MoE). Each epoch consisted of experience accumulation for 51’200 steps, gathered in total

from all environments, followed by 10 rounds of policy optimization using PPO [57]. All relevant hyperparameters were based on [39] with the exception of the policy variance, which we described in Section 3.5, and are available in the Supp. Material. The simulation runs at 150 Hz, while the control policy runs at 30 Hz, meaning that the control signal is repeated for 5 simulation frames.

**Datasets.** We trained KINESIS on the training split of the curated KIT-Locomotion dataset, consisting of 975 motions and five locomotion skills (walking, walking while turning, turning around in place, walking backwards, running). We evaluated the learned policy on the test split, containing 109 unseen motions from the same skill categories. For text-to-motion validation, we used MDM to generate synthetic motion trajectories for each skill category. Text prompts were chosen to ensure that generated motions matched the learned skills in style and velocity.

**Evaluation Metrics.** We report the motion imitation frame coverage as the percentage of the dataset (in frames) that the model successfully imitates. We also report the trial success rate, considering a trial successful when the tracked body markers of the model remain within 0.5 meters of the reference motion on average, throughout the trial trajectory. Furthermore, we report the global mean per-joint position error (MPJPE) in millimeters, averaged across all frames. All motion imitation experiments were performed three times. In the target goal-reaching task, we simulated 1000 random trials, and considered successful those trials that ended with the model within 0.1 meters of the target.

### 4.1. Motion Imitation

**Performance on KIT-locomotion Dataset.** A control policy trained using negative mining and three motor ex-

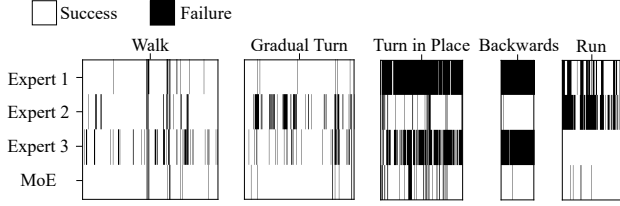


Figure 5. Performance heatmap of learned motions by different policy modules, clustered by locomotion skill and sorted by motion description.

parts combined with a MoE module achieved high performance on all locomotion skills (Table 2, see Supp. Material for a breakdown among experts). In four out of five skills, the model showed near-perfect performance in terms of frame coverage, while it could successfully imitate most trajectories of the dynamic “turn in place” skill.

**Skill specialization through negative mining.** To elucidate how the negative mining strategy produces generalist policies that conquer many skills, we analyzed the performance for each expert network individually (Figure 5). Our analysis highlights that the policy follows an implicit learning curriculum based on skill difficulty: the first expert learns how to walk forward and gradually turn, with moderate success in some running motions and no success in the two more difficulty skills. In turn, expert 2 focuses on the unconquered skills, and learns how to turn in place and walk backwards. This comes at a cost, as expert 2 regresses on some running and turning motions. In the third step, the final expert acquires a skill set that is virtually complementary to expert 2; given that it initializes from the previous weights, this is another instance of catastrophic forgetting. However, the gating network learns how to efficiently combine all 3 experts, leading to a high success rate for all skill types.

**Text-to-motion Imitation.** We prompted MDM with textual descriptions of simple locomotion (e.g., “the person walked in a circle slowly”). We then mapped the generated motion trajectories to a neutral SMPL model and use them as input to the control policy. KINESIS could successfully imitate examples in a zero-shot manner (Figure 4), although with reduced accuracy compared to the KIT-LoComotion dataset, with an average frame coverage of  $92.42 \pm 1.9\%$ , an average success rate of  $73.09 \pm 4.84\%$ , and an average MPJPE of  $98.95 \pm 6.25$  across 50 different motions ( $N=10$  runs per motion). More examples, including failure cases, are presented in the Supp. Material.

We demonstrate that KINESIS successfully imitates synthetic motions in a zero-shot manner, highlighting the robustness of the policy to noisy and imperfect input. Two

examples of text-to-motion imitation are shown in Figure 4. More examples, including failure cases, are available in the Supp. Material.

## 4.2. High-level Control Tasks

**Target Goal Reaching.** To test whether the locomotion skills acquired by KINESIS during motion imitation training can be transferred to other tasks without relying on high-quality reference data, we designed a target goal-reaching task. The objective of this task was for the model to reach a designated position from a random initial pose and facing direction. Starting positions were sampled from the KIT-LoComotion dataset, and targets were selected uniformly at random. Similar to the motion imitation task, the model received proprioceptive input, but the target pose was always set as the current pose, except for the root coordinates, which matched the target position. The model’s challenge was to reach the target without explicit guidance on how to execute the movement. By fine-tuning an expert policy for the new task, KINESIS consistently navigated to the target and remained there for the duration of the episode, achieving a 95.4% success rate (Figure 6). Notably, KINESIS utilized not only the locomotion skills acquired during the original imitation learning, but also additional skills it had not previously encountered, such as side steps and diagonal backward motion.

Importantly, the purpose of this task was not solely to learn a new skill, but to demonstrate the capacity of KINESIS to generate novel, human-like behavior. To emphasize this, we trained a baseline PPO policy with the same architecture from scratch, omitting the motion imitation stage. Although this baseline policy reached the target with a high, albeit lower success rate of 84.3%, it did so in an unrealistic manner that did not resemble human movement. A more detailed comparison is presented in the Supp. Material.

**Real-time Directional Control.** The target goal-reaching task demonstrated that KINESIS could break free of the constraints of motion imitation and apply its knowledge of the structure of human motion to high-level tasks. To further illustrate this capacity, we designed a variation of the goal-reaching environment, where the target was placed a few centimeters away from the model, simulating a carrot-on-a-stick scenario. This setup allowed for interactive, real-time changes to the target’s direction and distance from the agent. We observed that, without any additional training, KINESIS was able to walk towards the target indefinitely, demonstrating diverse locomotion skills like side and backwards steps (Figure 6). Additionally, the model adapted to changes in target distance by adjusting its speed accordingly. Details of these tasks and comparisons with the baseline policy are provided in the Supp. Material.

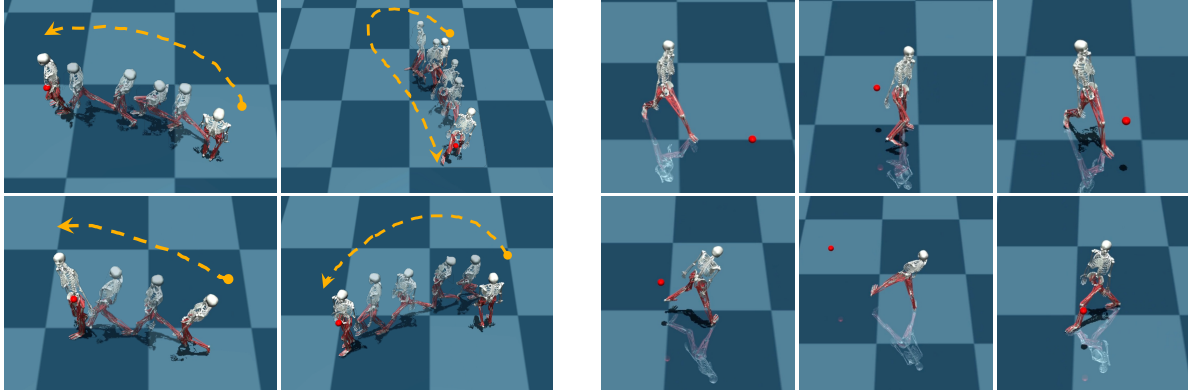


Figure 6. Examples of musculoskeletal motor control during high-level tasks. **Left:** *Target goal reaching*—intermediate poses along the trajectory are shown slightly transparent and follow the yellow arrows. **Right:** *Real-time directional control*—the distance of the red sphere determines the speed of the motion. Check out the Supp. Material for the corresponding videos.

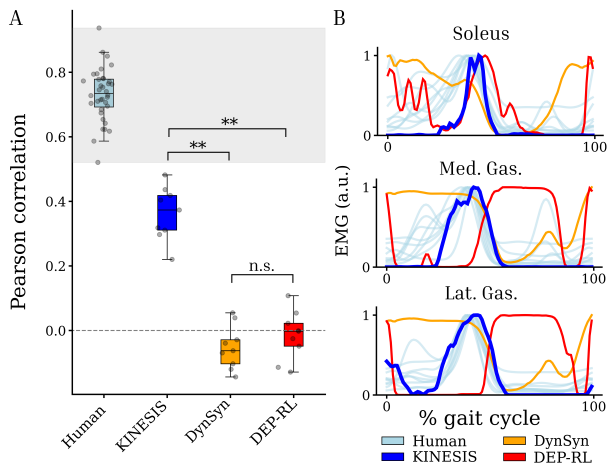


Figure 7. Correlation of generated gait-averaged muscle activity patterns with recorded human EMG data. **A:** When averaging over gait cycles and muscles, the correlation of muscle activity patterns produced by KINESIS with EMG data is significantly higher compared to alternative methods using the same musculoskeletal model (Wilcoxon signed-rank test,  $p = 0.004$ ). Individual points denote the average muscle activity correlation between the model and one subject ( $N = 9$ ). The upper-bound zone, shown in gray, is calculated based on the cross-human variability, here computed as the pairwise correlation between subjects ( $N = 36$ ). **B:** Example gait-averaged muscle activity patterns, where KINESIS is able to reproduce the qualitative characteristics (peaks and troughs) of the real EMG signals.

## 5. Comparison to human muscle dynamics (EMG)

Imitation performance and downstream controllability are great challenges to test the capacity of models of human motion. Nevertheless, a true understanding of human mo-

tor control necessitates that these models also capture the causal mechanisms of biological motion generation, which are the muscle activity patterns [37]. To assess how closely muscle-based control policies mimic real muscle control, we developed a benchmark that measures the correlation of generated muscle activity with recorded human electromyography (EMG) measurements. For this evaluation, we used a public dataset that includes recordings from nine leg muscles in nine different subjects during forward locomotion [71]. We compared KINESIS with two recent locomotion baselines, DynSyn and DEP-RL [23, 58], that use the same musculoskeletal model (MyoLeg). These methods were explicitly trained to move with a speed of 4.32 km/h (in the MyoWalk environment), whereas KINESIS can move at any speed on demand; to make comparisons fair, we also recorded KINESIS at that speed, and we used the closest available speed for the human data (4.5 km/h).

First, we measured the inherent variability across human subjects by averaging the individual muscle activity patterns across the periodic gait cycle [32, 71], and calculating the pair-wise Pearson correlation (Figure 7A). We considered this correlation range to represent a strong upper bound for model performance, since a model within that range would be just as good as another human’s muscle dynamics for predicting muscle activity. Computing the correlation of generated average activity patterns with the nine human subjects, we found that KINESIS achieves positive correlation and significantly outperforms both baselines for every subject; in contrast, the baselines fail to exceed 0 correlation for many subjects. In addition, when looking at the level of individual muscles, KINESIS is able to capture the qualitative characteristics of the activity patterns of muscles; the muscles shown in Figure 7B are especially relevant for identifying gait disorders [35]. Further results for all muscles, including failure cases, are included in the Supp. Material.

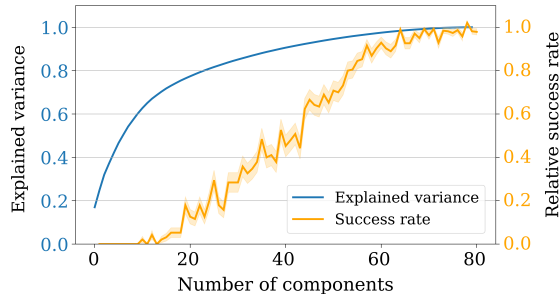


Figure 8. Comparison of two different methods for assessing control signal dimensionality. Dimensionality reduction (blue) overestimates the role of early principal components, which are insufficient to carry out the motor task (orange). The orange shaded region represents the 95% confidence interval based on 300 trials.

## 6. Motor Synergies for Locomotion

The correlation between human EMG data and muscle activity generated by KINESIS implies that our proposed model captures at least part of the causal link between motor control and behavior. Therefore, we can leverage KINESIS as an *in silico* model of the human sensorimotor system to tackle fundamental questions about motor control. One of these questions is how the human nervous system overcomes and potentially benefits from the over-actuated and high-dimensional nature of the musculoskeletal system (known as the “Bernstein problem” [3, 37]).

Previous studies have shown that a low number of components, commonly referred to as “muscle synergies”, are sufficient to account for a large proportion of the explained variance (EV) of EMG signals during motor tasks [14, 67, 68]. These results have led, according to some researchers, to the influential hypothesis that the brain “copes” with the complexity of motor control by actually only controlling a few synergies; this idea has also been formalized to create “brain-inspired” control policies of humanoid characters [2, 20, 23]. However, techniques that focus solely on explaining the variance of the motor control ignore the possibility that small errors in the muscle control signal could lead to catastrophic failure in terms of task performance [37]. Therefore, instead of the common signal reconstruction metric, it is much more informative to quantify the dimensionality of a control signal by the number of components that are required to retrieve full task performance [9].

To this end, we recorded the muscle activity patterns generated by KINESIS during the target goal reaching task, and we decomposed it using Principal Component Analysis. Like in many previous studies, we observed that a relatively low number of components was sufficient to explain a significant proportion of the signal’s EV (Figure 8). We then repeated the task, this time projecting the control signal onto a subspace of principal components before providing

it to the model (see Chiappa et al. for the inspiration for this method used for dexterous hand use). We found that the task performance was only recovered when using a much higher number of components. This highlights that for task success, almost all dimensions are required (Figure 8). Overall, these results show that embodied musculoskeletal policies, such as KINESIS, can provide a powerful alternative to traditional methods of investigating human motor control.

## 7. Discussion and Limitations

We presented a RL-based motion imitation framework for the control of a lower-body musculoskeletal model. KINESIS, our trained policy, shows high imitation performance on 1.9 hours of MoCap sequences, tackles text-to-motion prompts, and can be controlled interactively. More importantly, to the best of our knowledge, KINESIS is the first model-free musculoskeletal control policy that combines diverse locomotion skills and generates muscle activation patterns that approximate real human EMG recordings, without being explicitly trained to do so. While the lack of upper body control arguably makes these feats more impressive, it also places constraints on the diversity of the feasible motion repertoire. Additionally, the current proprioceptive feedback is idealized such that sensory information is conveyed instantaneously and noise-free to the control policy [37, 70]. In the future, we aim to incorporate sensory and motor noise to enhance the robustness of the policy and enable it to tackle noisy reference motions and more complex environments. We will deploy KINESIS on additional musculoskeletal models, such as the MyoArm [4, 6], and the (hopefully) soon-to-be-released full-body model.

**Acknowledgments:** We thank members of the Mathis Group for helpful feedback. In particular, we thank Bianca Ziliotto, Chengkun Li and Alessandro Marin Vargas for feedback on earlier versions of this article. This project was funded by Swiss SNF grant (310030\_212516).

## References

- [1] Jake K Aggarwal and Quin Cai. Human Motion Analysis: A Review. *Computer Vision and Image Understanding*, 73(3): 428–440, 1999. 1
- [2] Cameron Berg, Vittorio Caggiano, and Vikash Kumar. SAR: generalization of physiological agility and dexterity via synergistic action representation. *Autonomous Robots*, 48(8):28, 2024. 2, 9
- [3] Nikolai A. Bernstein. *The co-ordination and regulation of movements*. Oxford, New York, Pergamon Press, 1967. 1, 2, 9
- [4] Vittorio Caggiano, Huawei Wang, Guillaume Durandau, Massimo Sartori, and Vikash Kumar. MyoSuite – A contact-rich simulation suite for musculoskeletal motor control. *arXiv preprint arXiv:2205.13600*, 2022. 2, 3, 9
- [5] Vittorio Caggiano, Huawei Wang, Guillaume Durandau, Seungmoon Song, Yuval Tassa, Massimo Sartori, and Vikash Kumar. MyoChallenge: Learning contact-rich manipulation using a musculoskeletal hand, 2022. 2
- [6] Vittorio Caggiano, Guillaume Durandau, Huawei Wang, Alberto Chiappa, Alexander Mathis, Pablo Tano, Nisheet Patel, Alexandre Pouget, Pierre Schumacher, Georg Martius, et al. MyoChallenge 2022: Learning contact-rich manipulation using a musculoskeletal hand. In *NeurIPS 2022 Competition Track*, pages 233–250. PMLR, 2023. 9
- [7] Vittorio Caggiano, Guillaume Durandau, Seungmoon Song, Chun Kwang Tan, Huiyi Wang, Balint Hodossy, Pierre Schumacher, Letizia Gionfrida, Massimo Sartori, and Vikash Kumar. Myochallenge 2024: Physiological dexterity and agility in bionic humans. In *NeurIPS 2024 Competition Track*, 2024.
- [8] Alberto Silvio Chiappa, Alessandro Marin Vargas, Ann Huang, and Alexander Mathis. Latent exploration for Reinforcement Learning. *Advances in Neural Information Processing Systems*, 36, 2024. 5
- [9] Alberto Silvio Chiappa, Pablo Tano, Nisheet Patel, Abigail Ingster, Alexandre Pouget, and Alexander Mathis. Acquiring musculoskeletal skills with curriculum-based reinforcement learning. *Neuron*, 112(23):3969–3983, 2024. 1, 2, 5, 9
- [10] Mia Chiquier and Carl Vondrick. Muscles in action. In *Proceedings of the IEEE/CVF International Conference on Computer Vision*, pages 22091–22101, 2023. 3
- [11] Erwin Coumans and Yunfei Bai. Pybullet, a python module for physics simulation for games, robotics and machine learning, 2016. 2
- [12] Abdelmoutaleb Dakri, Vaibhav Arora, Léo Challier, Marilyn Keller, Michael J Black, and Sergi Pujades. On predicting 3d bone locations inside the human body. In *International Conference on Medical Image Computing and Computer-Assisted Intervention*, pages 336–346. Springer, 2024. 1
- [13] Sudeep Dasari, Abhinav Gupta, and Vikash Kumar. Learning dexterous manipulation from exemplar object trajectories and pre-grasps. In *2023 IEEE International Conference on Robotics and Automation (ICRA)*, pages 3889–3896. IEEE, 2023. 1
- [14] Andrea d’Avella, Philippe Saltiel, and Emilio Bizzi. Combinations of muscle synergies in the construction of a natural motor behavior. *Nature neuroscience*, 6(3):300–308, 2003. 1, 2, 9
- [15] Scott L Delp, Frank C Anderson, Allison S Arnold, Peter Loan, Ayman Habib, Chand T John, Eran Guendelman, and Darryl G Thelen. Opensim: open-source software to create and analyze dynamic simulations of movement. *IEEE transactions on biomedical engineering*, 54(11):1940–1950, 2007. 1, 2, 3
- [16] Travis DeWolf, Steffen Schneider, Paul Soubiran, Adrian Roggenbach, and Mackenzie Mathis. Neuro-musculoskeletal modeling reveals muscle-level neural dynamics of adaptive learning in sensorimotor cortex. *bioRxiv*, pages 2024–09, 2024. 3
- [17] Taylor JM Dick, Kylie Tucker, François Hug, Manuela Besomi, Jaap H van Dieën, Roger M Enoka, Thor Besier, Richard G Carson, Edward A Clancy, Catherine Disselhorst-Klug, et al. Consensus for experimental design in electromyography (cede) project: Application of emg to estimate muscle force. *Journal of Electromyography and Kinesiology*, page 102910, 2024. 3
- [18] Ahmet Erdemir, Lealem Mulugeta, Joy P Ku, Andrew Drach, Marc Horner, Tina M Morrison, Grace CY Peng, Rajanikanth Vadigepalli, William W Lytton, and Jerry G Myers Jr. Credible practice of modeling and simulation in healthcare: ten rules from a multidisciplinary perspective. *Journal of translational medicine*, 18(1):369, 2020. 3
- [19] Yusen Feng, Xiyan Xu, and Libin Liu. Musclevae: Model-based controllers of muscle-actuated characters. In *SIGGRAPH Asia 2023 Conference Papers*, pages 1–11, 2023. 2, 3, 4
- [20] F Ficuciello, A Migliozzi, G Laudante, P Falco, and B Siciliano. Vision-based grasp learning of an anthropomorphic hand-arm system in a synergy-based control framework. *Science robotics*, 4(26):eaao4900, 2019. 9
- [21] Henri-Jacques Geiß, Firas Al-Hafez, Andre Seyfarth, Jan Peters, and Davide Tateo. Exciting action: Investigating efficient exploration for learning musculoskeletal humanoid locomotion. *arXiv preprint arXiv:2407.11658*, 2024. 5
- [22] Yoni Gozlan, Antoine Falisse, Scott Uhlrich, Anthony Gatti, Michael Black, and Akshay Chaudhari. Opencapbench: A benchmark to bridge pose estimation and biomechanics. *arXiv preprint arXiv:2406.09788*, 2024. 1
- [23] Kaibo He, Chenhui Zuo, Chengtian Ma, and Yanan Sui. Dynsyn: dynamical synergistic representation for efficient learning and control in overactuated embodied systems. *arXiv preprint arXiv:2407.11472*, 2024. 2, 3, 8, 9
- [24] Jennifer L Hicks, Michael H Schwartz, Allison S Arnold, and Scott L Delp. Crouched postures reduce the capacity of muscles to extend the hip and knee during the single-limb stance phase of gait. *Journal of biomechanics*, 41(5):960–967, 2008. 2
- [25] Jennifer L Hicks, Thomas K Uchida, Ajay Seth, Apoorva Rajagopal, and Scott L Delp. Is my model good enough? best practices for verification and validation of musculoskeletal models and simulations of movement. *Journal of biomechanical engineering*, 137(2):020905, 2015. 3

- [26] Archibald Vivian Hill. The heat of shortening and the dynamic constants of muscle. *Proceedings of the Royal Society of London. Series B-Biological Sciences*, 126(843):136–195, 1938. 2
- [27] Jemin Hwangbo, Joonho Lee, and Marco Hutter. Per-contact iteration method for solving contact dynamics. *IEEE Robotics and Automation Letters*, 3(2):895–902, 2018. 2
- [28] Robert A Jacobs, Michael I Jordan, Steven J Nowlan, and Geoffrey E Hinton. Adaptive mixtures of local experts. *Neural computation*, 3(1):79–87, 1991. 6
- [29] Jordan Juravsky, Yunrong Guo, Sanja Fidler, and Xue Bin Peng. Superpadl: Scaling language-directed physics-based control with progressive supervised distillation. In *ACM SIGGRAPH 2024 Conference Papers*, pages 1–11, 2024. 2
- [30] Łukasz Kidziński, Carmichael Ong, Sharada Prasanna Mohanty, Jennifer Hicks, Sean Carroll, Bo Zhou, Hongsheng Zeng, Fan Wang, Rongzhong Lian, Hao Tian, et al. Artificial intelligence for prosthetics: Challenge solutions. In *The NeurIPS’18 Competition: From Machine Learning to Intelligent Conversations*, pages 69–128. Springer, 2020. 2
- [31] Taku Komura, Yoshihisa Shinagawa, and Toshiyasu L Kunii. Creating and retargetting motion by the musculoskeletal human body model. *The visual computer*, 16:254–270, 2000. 3
- [32] Francesco Lacquaniti, Yuri P Ivanenko, and Myrka Zago. Patterned control of human locomotion. *The Journal of physiology*, 590(10):2189–2199, 2012. 8
- [33] Jeongseok Lee, Michael X. Grey, Sehoon Ha, Tobias Kunz, Sumit Jain, Yuting Ye, Siddhartha S. Srinivasa, Mike Stilman, and C Karen Liu. Dart: Dynamic animation and robotics toolkit. *The Journal of Open Source Software*, 3(22):500, 2018. 2, 3
- [34] Seunghwan Lee, Moonseok Park, Kyoungmin Lee, and Jehee Lee. Scalable muscle-actuated human simulation and control. *ACM Transactions On Graphics (TOG)*, 38(4):1–13, 2019. 2, 4
- [35] Rachel L Lenhart, Carrie A Francis, Amy L Lenz, and Darryl G Thelen. Empirical evaluation of gastrocnemius and soleus function during walking. *Journal of biomechanics*, 47(12):2969–2974, 2014. 8
- [36] Zhi-Yi Lin, Bofan Lyu, Judith Cueto Fernandez, Eline Van Der Kruk, Ajay Seth, and Xucong Zhang. 3d kinematics estimation from video with a biomechanical model and synthetic training data. In *Proceedings of the IEEE/CVF Conference on Computer Vision and Pattern Recognition*, pages 1441–1450, 2024. 3
- [37] Gerald E Loeb. Learning to use muscles. *Journal of human kinetics*, 76:9, 2021. 1, 2, 3, 8, 9
- [38] Matthew Loper, Naureen Mahmood, Javier Romero, Gerard Pons-Moll, and Michael J. Black. *SMPL: A Skinned Multi-Person Linear Model*, pages 851–866. Association for Computing Machinery, 2023. 3, 13
- [39] Zhengyi Luo, Jinkun Cao, Kris Kitani, Weipeng Xu, et al. Perpetual humanoid control for real-time simulated avatars. In *Proceedings of the IEEE/CVF International Conference on Computer Vision*, pages 10895–10904, 2023. 1, 2, 4, 5, 6, 13
- [40] Zhengyi Luo, Jinkun Cao, Josh Merel, Alexander Winkler, Jing Huang, Kris Kitani, and Weipeng Xu. Universal humanoid motion representations for physics-based control. *arXiv preprint arXiv:2310.04582*, 2023. 1, 2, 4, 5
- [41] Naureen Mahmood, Nima Ghorbani, Nikolaus F. Troje, Gerard Pons-Moll, and Michael J. Black. AMASS: Archive of motion capture as surface shapes. In *International Conference on Computer Vision*, pages 5442–5451, 2019. 3, 13
- [42] Viktor Makoviychuk, Lukasz Wawrzyniak, Yunrong Guo, Michelle Lu, Kier Storey, Miles Macklin, David Hoeller, Nikita Rudin, Arthur Allshire, Ankur Handa, et al. Isaac gym: High performance gpu-based physics simulation for robot learning. *arXiv preprint arXiv:2108.10470*, 2021. 2
- [43] Christian Mandery, Ömer Terlemez, Martin Do, Nikolaus Vahrenkamp, and Tamim Asfour. The kit whole-body human motion database. In *2015 International Conference on Advanced Robotics (ICAR)*, pages 329–336. IEEE, 2015. 13
- [44] Mackenzie Weygandt Mathis, Adriana Perez Rotondo, Edward F Chang, Andreas S Tolia, and Alexander Mathis. Decoding the brain: From neural representations to mechanistic models. *Cell*, 187(21):5814–5832, 2024. 1, 3
- [45] Ashvin Nair, Bob McGrew, Marcin Andrychowicz, Wojciech Zaremba, and Pieter Abbeel. Overcoming exploration in reinforcement learning with demonstrations. In *2018 IEEE international conference on robotics and automation (ICRA)*, pages 6292–6299. IEEE, 2018. 2
- [46] Ali Nasr, Kevin Zhu, and John McPhee. Using musculoskeletal models to generate physically-consistent data for 3d human pose, kinematic, dynamic, and muscle estimation. *Multibody System Dynamics*, pages 1–34, 2024. 3
- [47] Jungnam Park, Sehee Min, Phil Sik Chang, Jaedong Lee, Moon Seok Park, and Jehee Lee. Generative gaitnet. In *ACM SIGGRAPH 2022 Conference Proceedings*, pages 1–9, 2022. 2
- [48] Xue Bin Peng, Glen Berseth, and Michiel Van de Panne. Terrain-adaptive locomotion skills using deep reinforcement learning. *ACM Transactions on Graphics (TOG)*, 35(4):1–12, 2016. 2
- [49] Xue Bin Peng, Pieter Abbeel, Sergey Levine, and Michiel Van de Panne. Deepmimic: Example-guided deep reinforcement learning of physics-based character skills. *ACM Transactions On Graphics (TOG)*, 37(4):1–14, 2018. 2, 4
- [50] Xue Bin Peng, Ze Ma, Pieter Abbeel, Sergey Levine, and Angjoo Kanazawa. Amp: Adversarial motion priors for stylized physics-based character control. *ACM Transactions on Graphics (ToG)*, 40(4):1–20, 2021. 2
- [51] Xue Bin Peng, Yunrong Guo, Lina Halper, Sergey Levine, and Sanja Fidler. Ase: Large-scale reusable adversarial skill embeddings for physically simulated characters. *ACM Transactions On Graphics (TOG)*, 41(4):1–17, 2022. 2
- [52] Matthias Plappert, Christian Mandery, and Tamim Asfour. The kit motion-language dataset. *Big data*, 4(4):236–252, 2016. 2, 3
- [53] Wenhui Qin, Ran Tao, Libo Sun, and Kaiyue Dong. Muscle-driven virtual human motion generation approach based on deep reinforcement learning. *Computer Animation and Virtual Worlds*, 33(3-4):e2092, 2022. 2, 3

- [54] Apoorva Rajagopal, Christopher L Dembia, Matthew S Demers, Denny D Delp, Jennifer L Hicks, and Scott L Delp. Full-body musculoskeletal model for muscle-driven simulation of human gait. *IEEE transactions on biomedical engineering*, 63(10):2068–2079, 2016. 2, 3
- [55] Aravind Rajeswaran, Vikash Kumar, Abhishek Gupta, Giulia Vezzani, John Schulman, Emanuel Todorov, and Sergey Levine. Learning complex dexterous manipulation with deep reinforcement learning and demonstrations. *arXiv preprint arXiv:1709.10087*, 2017. 2
- [56] Azhar Aulia Saputra, Chin Wei Hong, Tadimitsu Matsuda, and Naoyuki Kubota. A real-time control system of upper-limb human musculoskeletal model with environmental integration. *IEEE access*, 2023. 3
- [57] John Schulman, Filip Wolski, Prafulla Dhariwal, Alec Radford, and Oleg Klimov. Proximal policy optimization algorithms. *arXiv preprint arXiv:1707.06347*, 2017. 5, 6
- [58] Pierre Schumacher, Daniel Häufle, Dieter Büchler, Syn Schmitt, and Georg Martius. Dep-rl: Embodied exploration for reinforcement learning in overactuated and musculoskeletal systems. *arXiv preprint arXiv:2206.00484*, 2022. 2, 3, 8
- [59] Pierre Schumacher, Thomas Geijtenbeek, Vittorio Caggiano, Vikash Kumar, Syn Schmitt, Georg Martius, and Daniel FB Haeufle. Emergence of natural and robust bipedal walking by learning from biologically plausible objectives. *iScience*, 2025. 2
- [60] Ajay Seth, Jennifer L Hicks, Thomas K Uchida, Ayman Habib, Christopher L Dembia, James J Dunne, Carmichael F Ong, Matthew S DeMers, Apoorva Rajagopal, Matthew Millard, et al. Opensim: Simulating musculoskeletal dynamics and neuromuscular control to study human and animal movement. *PLoS computational biology*, 14(7):e1006223, 2018. 2
- [61] Dana Sharon and Michiel van de Panne. Synthesis of controllers for stylized planar bipedal walking. In *Proceedings of the 2005 IEEE International Conference on Robotics and Automation*, pages 2387–2392. IEEE, 2005. 2
- [62] Seungmoon Song, Łukasz Kidziński, Xue Bin Peng, Carmichael Ong, Jennifer Hicks, Sergey Levine, Christopher G Atkeson, and Scott L Delp. Deep reinforcement learning for modeling human locomotion control in neuromechanical simulation. *Journal of neuroengineering and rehabilitation*, 18:1–17, 2021. 1, 2, 3
- [63] Chen Tessler, Yoni Kasten, Yunrong Guo, Shie Mannor, Gal Chechik, and Xue Bin Peng. Calm: Conditional adversarial latent models for directable virtual characters. In *ACM SIGGRAPH 2023 Conference Proceedings*, pages 1–9, 2023. 2
- [64] Chen Tessler, Yunrong Guo, Ofir Nabati, Gal Chechik, and Xue Bin Peng. Maskedmimic: Unified physics-based character control through masked motion inpainting. *arXiv preprint arXiv:2409.14393*, 2024. 1, 2
- [65] Guy Tevet, Sigal Raab, Brian Gordon, Yoni Shafir, Daniel Cohen-or, and Amit Haim Bermano. Human motion diffusion model. In *The Eleventh International Conference on Learning Representations*, 2023. 6, 13
- [66] Emanuel Todorov, Tom Erez, and Yuval Tassa. Mujoco: A physics engine for model-based control. In *2012 IEEE/RSJ international conference on intelligent robots and systems*, pages 5026–5033. IEEE, 2012. 2, 3
- [67] Matthew C Tresch and Anthony Jarc. The case for and against muscle synergies. *Current opinion in neurobiology*, 19(6):601–607, 2009. 9
- [68] Matthew C Tresch, Vincent CK Cheung, and Andrea d’Avella. Matrix factorization algorithms for the identification of muscle synergies: evaluation on simulated and experimental data sets. *Journal of neurophysiology*, 95(4):2199–2212, 2006. 9
- [69] Michael T Turvey. Coordination. *American psychologist*, 45(8):938, 1990. 1
- [70] Alessandro Marin Vargas, Axel Bisi, Alberto S Chiappa, Chris Versteeg, Lee E Miller, and Alexander Mathis. Task-driven neural network models predict neural dynamics of proprioception. *Cell*, 187(7):1745–1761, 2024. 9
- [71] Huawei Wang, Akash Basu, Guillaume Durandau, and Massimo Sartori. A wearable real-time kinetic measurement sensor setup for human locomotion. *Wearable technologies*, 4:e11, 2023. 3, 8
- [72] Keenon Werling, Nicholas A Bianco, Michael Raitor, Jon Stingel, Jennifer L Hicks, Steven H Collins, Scott L Delp, and C Karen Liu. Addbiomechanics: Automating model scaling, inverse kinematics, and inverse dynamics from human motion data through sequential optimization. *Plos one*, 18(11):e0295152, 2023. 2, 3
- [73] Jungdam Won, Deepak Gopinath, and Jessica Hodgins. Physics-based character controllers using conditional vaes. *ACM Transactions on Graphics (TOG)*, 41(4):1–12, 2022. 13
- [74] Heyuan Yao, Zhenhua Song, Baoquan Chen, and Libin Liu. Controlvae: Model-based learning of generative controllers for physics-based characters. *ACM Transactions on Graphics (TOG)*, 41(6):1–16, 2022. 2
- [75] Felix E Zajac. Muscle and tendon: properties, models, scaling, and application to biomechanics and motor control. *Critical reviews in biomedical engineering*, 17(4):359–411, 1989. 2
- [76] Chenhui Zuo, Kaibo He, Jing Shao, and Yanan Sui. Self model for embodied intelligence: Modeling full-body human musculoskeletal system and locomotion control with hierarchical low-dimensional representation. In *2024 IEEE International Conference on Robotics and Automation (ICRA)*, pages 13062–13069. IEEE, 2024. 2

## Motion Imitation: Data Processing

To ensure compatibility with the skeletal models, the KIT Dataset is extracted from the AMASS motion capture (MoCap) archive [41, 43]. Each motion consists of a textual description, video and body shape metadata, and motion data in numerical array form. The key motion data necessary to process the motion are the “poses” data, which contain the SMPL-H pose in axis-angle space [38], and the “trans” data, which contain the global root translation at each frame.

We follow Luo et al. to align the KIT motions to the correct skeletal reference frame [39]. First, we perform down-sampling to reduce the MoCap frame rate from 100 to 30 frames per second (FPS). Then, we map the SMPL body joints to 24 joints of a template skeleton model in Mujoco, which shares the same dimensions as the MyoLeg musculoskeletal model. We transform the joint rotations from their axis-angle representation to quaternions. Following that, we implement these rotations on the template skeleton model, and compute the global rotation of each joint. Finally, we rotate the skeleton such that the z-axis vector is pointing upwards, and extract the transformed local joint rotations.

### Text-to-motion

We use the Human Motion Diffusion Model (MDM) by Tevet et al. to generate text-conditioned motion sequences resembling the fundamental locomotion skills that KINESIS learns during motion imitation. In particular, we use five textual prompts and generate 10 samples for each one, totaling 50 motions:

- “the person walked forward”,
- “the person turned left”,
- “the person turned right”,
- “the person walked in a circle slowly”,
- “the person walked backward slowly”.

Each motion has a duration of three seconds. We provide evaluation statistics for each prompt (Table S1), and we encourage readers to refer to the supplementary videos for demonstrations and failure cases.

### High-Level Control

When fine-tuning KINESIS for high-level control, we keep the same structure for the observations and the policy outputs. More specifically, we provide the policy with proprioceptive input and target keypoints, but we set all “targets” to the current position of the respective body part, apart from the target root position, which is set to the target position, similar to [39]. During the fine-tuning phase, the target position is randomly sampled from within a 2-by-2  $m^2$  area, and the musculoskeletal model is initialized at a random pose sampled from the KIT-Locomotion dataset. We update the reward function to better match the high-level task

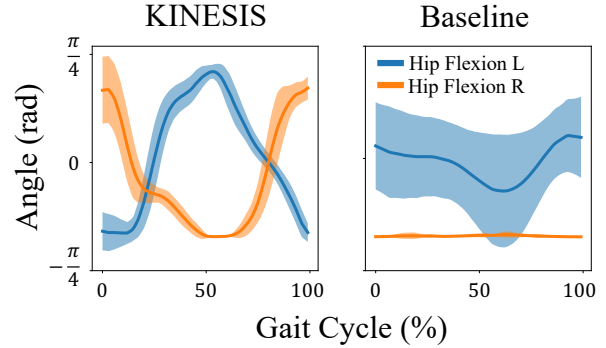


Figure S1. Joint angle analysis: KINESIS produces human-like, symmetric motion where both legs move in a cyclical fashion, as indicated by the average hip flexion along the gait cycle. In contrast, the baseline policy produces unrealistic motion where the right leg is still, while the left leg “drags” the body forward. Shaded areas indicate standard deviation. Data were recorded during forward motion over a period of 30 seconds for each policy.

by replacing the position and tracking velocity rewards with two new components:

$$r_t^{track} = \delta_{t-1} - \delta_t, \quad (8)$$

$$r_t^{success} = \mathbb{1}_{\{\delta_t < 0.1\}}, \quad (9)$$

where  $\delta_t$  denotes the distance between the root and the target position at time  $t$ , which is inspired by Won et al.. We set the duration of each episode to 150 frames (5 seconds), and terminate the episode early if the height of the root drops below 0.7 meters, indicating that the musculoskeletal model has lost its balance.

To reach a high performance in the target goal reaching task, we used the second expert policy from KINESIS and trained on the new task for 5’000 additional epochs. The baseline policy, which used the same architecture as the KINESIS experts, also trained on the target reaching task for 5’000 epochs, skipping the motion imitation training. While the baseline model learns to stand upright and moves towards the target, it employs an unrealistic motion strategy in which one leg is stiff and on the ground, and the other leg is used to propel the model forward (Figure S1). We refer the reader to the Supplementary Videos for a demonstration of both policies on the two high-level control tasks.

### Comparison to EMG

Figure S2 shows an expanded comparison of generated muscle activity with real EMG for individual muscles. We observed that KINESIS is positively correlated with all muscles except the vastus lateralis, which interestingly shows very low and sometimes negative correlation even across human subjects. Results are also modest for the rec-

Table S1. Quantitative motion imitation results on text-to-motion generated sequences, evaluated zero-shot. Each prompt was used to generate 10 motion sequences, and each motion was tested 10 times. Mean and SEM for N=10 trials.

Prompt	Frame Coverage $\uparrow$	Success $\uparrow$	$E_{MPJPE} \downarrow$
The person walked <b>backward</b> slowly	94.32 $\pm$ 3.65 %	77.00 $\pm$ 10.96 %	97.62 $\pm$ 10.59
The person <b>turned left</b>	94.00 $\pm$ 3.47 %	71.00 $\pm$ 14.03 %	79.90 $\pm$ 13.36
The person <b>turned right</b>	99.80 $\pm$ 0.19 %	99.00 $\pm$ 0.95 %	65.70 $\pm$ 4.37
The person <b>walked in a circle</b> slowly	82.54 $\pm$ 6.74 %	53.64 $\pm$ 10.62 %	139.00 $\pm$ 14.85
The person <b>walked forward</b>	95.50 $\pm$ 1.61 %	81.00 $\pm$ 5.91 %	94.50 $\pm$ 11.39

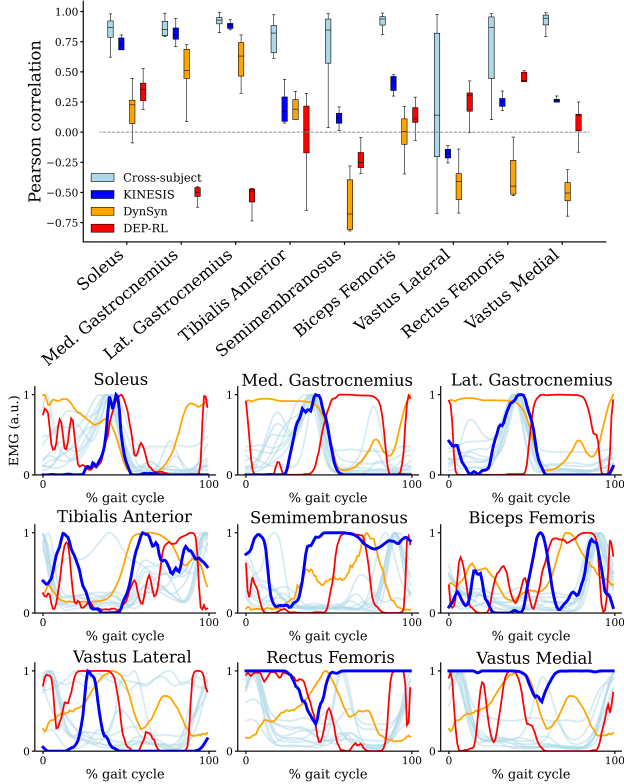


Figure S2. **Top:** Correlation of generated gait-averaged muscle activity patterns with recorded human data, shown individually for each muscle for which human data was available. **Bottom:** The gait-averaged muscle activity patterns shown on top of real EMG signals.

tus femoris and vastus medialis muscles, where KINESIS generates high activity across the entire gait cycle.

## Reinforcement Learning: Hyperparameters

Hyperparameters used to train KINESIS can be found in Table S2.

Table S2. KINESIS: Hyperparameters

Hyperparameter	Value
Sim. timestep	1/150
Control interval	5
PD controller $k_p$	1
PD controller $k_d$	1
Transformer layers	2
Reward $k_{pos}$	200
Reward $k_{vel}$	5
Reward $k_{up}$	3
Reward $w_{pos}$	0.6
Reward $w_{vel}$	0.2
Reward $w_e$	0.1
Reward $w_{up}$	0.1
Reward $w_{tracking}$	0.8
Reward $w_{success}$	20
PPO $\gamma$	0.99
PPO $\epsilon$	0.2
PPO $\tau$	0.95
PPO learning rate	$5 \times 10^{-5}$
PPO optimizer	Adam
Activation function	SiLU